Highlights

Boundary plasma studies for a spherical tokamak with lithium walls
A. Antony, L. Carbajal, T. D. Rognlien, M. V. Umansky, A. Froese, S. Howard, C. Ribeiro, R. Ivanov, C. Dunlea, C. P. McNally
• First edge modelling study of General Fusion's PI3 spherical tokamak
 Exploring the impact of limiter insertion depth on lithium- coated spherical tokamak
• Limiter location effects
Diverted compared with limited and diverted
Diversed compared with inflited and diversed

Boundary plasma studies for a spherical tokamak with lithium walls

A. Antony^{a,*}, L. Carbajal^a, T. D. Rognlien^b, M. V. Umansky^b, A. Froese^a, S. Howard^a, C. Ribeiro^a, R. Ivanov^a, C. Dunlea^a, C. P. McNally^a

^aGeneral Fusion, 6020 Russ Baker Way, Richmond, V7B 1B4, BC, Canada
^bLawrence Livermore National Laboratory, Livermore, 94551, CA, USA

Abstract

Boundary plasma and plasma-material interactions are investigated for magnetised target fusion (MTF) applications. The General Fusion magnetised target fusion technology uses coaxial helicity injection (CHI) start-up which forms a spherical tokamak in a cavity with liquid lithium walls that will subsequently be compressed to fusion conditions [1]. The Plasma Injector 3 (PI3) experiment at General Fusion is a non-compressing experiment with solid lithium walls that studies the formation and quasi-steady state operation of a CHI spherical tokamak [2]. An explorative study is carried out for wall-limited versus diverted configurations for PI3 using the fluid edge transport code UEDGE. Experimental edge temperature and density profiles from triple Langmuir probes are utilized to set up realistic plasma profiles in UEDGE. In UEDGE, we model the wall-limited plasma via a thin limiter with various insertion depths. It is found that limiter depth and location are key parameters in determining radial profiles and sputtered lithium behaviour. Furthermore, it is found that the overall sputtering of the limiter is significantly lower than the sputtering of the wall in some of the limiter configurations studied. Lithium impurity and neutral behaviour are compared between limited and diverted configurations.

Keywords: Plasma-Surface interaction, Divertor, Limiter, Heat Flux, Magnetised Target Fusion

1. Introduction

General Fusion creates spherical tokamak (ST) target plasmas using the third generation of its coaxial helicity injector, PI3, to study the stability and confinement of ST target in the presence of lithium walls.

Early theoretical and numerical studies on the use of solid and liquid lithium as the first wall of standard magnetised confinement fusion (MCF) devices suggested that lithium walls would provide benefits such as more stable plasmas with higher and flatter electron and ion temperature profiles in the core plasma [3, 4] due to the low recycling of hydrogenic neutrals from the lithium walls. This has been experimentally observed in various experimental fusion devices, such as in the NSTX spherical tokamak that used lithium-coated graphite walls[5, 6, 7], the LTX tokamak that used solid and liquid lithium walls [8, 9], and the EAST tokamak that used solid lithium walls, puffed lithium powder into the plasma [10, 11] and performed extensive studies on a liquid lithium limiter [11, 12].

Modelling and simulation of lithium transport in fusion plasmas include the use of codes that solve the local neoclassical transport of impurities given a background plasma and transport coefficients [13, 14] such as NCLASS [15], NEO [16], and MIST [17] that solve for the impurity profiles including atomic processes of ionisation and recombination, MHD and

 ${\it Email address:} \ {\tt abetharan.antony@generalfusion.com} \ (A. \ Antony)$

edge codes such as EMC3 [18], UEDGE [19], and SOLPS [20] that solve the background plasma (main hydrogenic ions and electrons) and use either a fluid description for impurities that evolves consistently with the background plasma or a kinetic description of impurities through coupling to codes such as EIRENE [21] or DEGAS2 [22] that solve for the guidingcentre orbits of impurities including atomic physics and collisions with the background plasma. More detailed modelling and simulation of the transport of other impurities, such as carbon, in fusion experiments solve for the drift-kinetic dynamics of the main hydrogenic ions, electrons, and impurities, allowing the inclusion of anomalous transport coefficients. Examples of this type of modelling are the XGC0 and XGC1 codes [23, 13]. However, it is noted that this latter approach may result in very expensive simulations that prevent the extensive application of this approach.

PI3 routinely operates in a magnetic configuration where particle and heat fluxes from the core will deposit to divertor and inboard limiter surfaces. This allows for exploring the effects of fluxes to multiple surfaces on edge and plasma performance concerning neutral and lithium impurity behaviour. This is not an operating mode unique to PI3, but also occurs in tokamaks, where particle and heat fluxes will impact various surfaces such as the centre-post and baffles near the x-point whilst simultaneously being diverted.

To model this, we insert a thin plate limiter in a divertor configuration and examine the edge behaviour. We study the impact of various plasma configurations in PI3 ranging from only diverted to multiple thin plate limiter scenarios that are possi-

^{*}Corresponding author

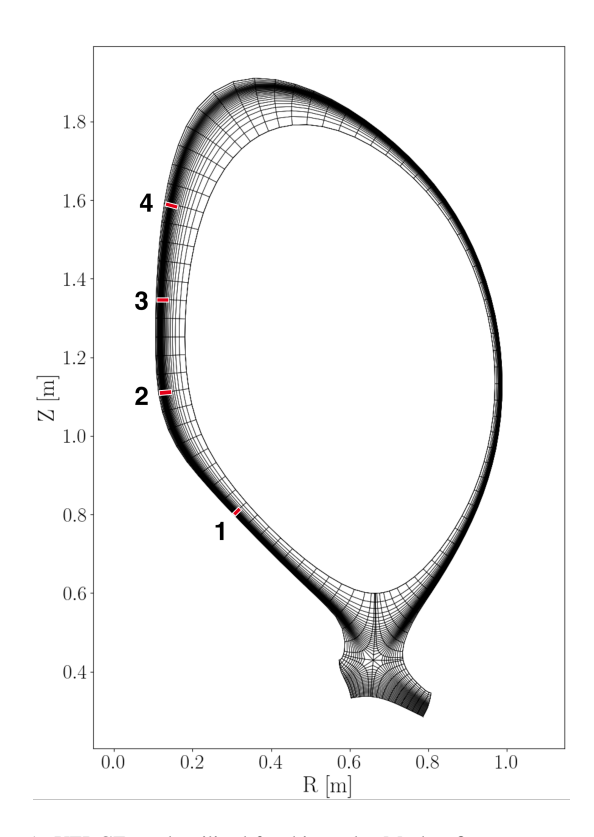


Figure 1: UEDGE mesh utilised for this study. Mesh refinement was not applied. Locations of the limiter are highlighted for the four poloidal locations studied.

bly expected on PI3 and indeed on other tokamaks of equivalent size using the edge code UEDGE [19]. This study provides valuable information for understanding typical edge behaviour resulting from fluxes depositing on limiter and divertor surfaces in the presence of lithium-coated walls. We present three separate studies: 1) Limiter insertion depth effect, 2) The impact of limiter location and 3) Purely diverted compared with limited inboard operation. Finally, we present early design studies for a plasma compression device.

2. Simulation Setup

We utilise the edge code UEDGE to solve the 2D fluid equations for the hydrogenic and impurity species. The impurity momentum equations are solved with an assumption of force balance and are flux-limited in the radial and poloidal directions. Furthermore, parallel thermal transport is flux-limited. Additional details of the equations solved can be found in [19, 24]. Recently recommissioned UEDGE features are utilised in this work:

- Thin Plate Limiters
- Evaporation from Limiter
- Sputtering from Limiter

In addition to the thin plater limiter, UEDGE has recently been upgraded to model fully or partially limited tokamaks via a

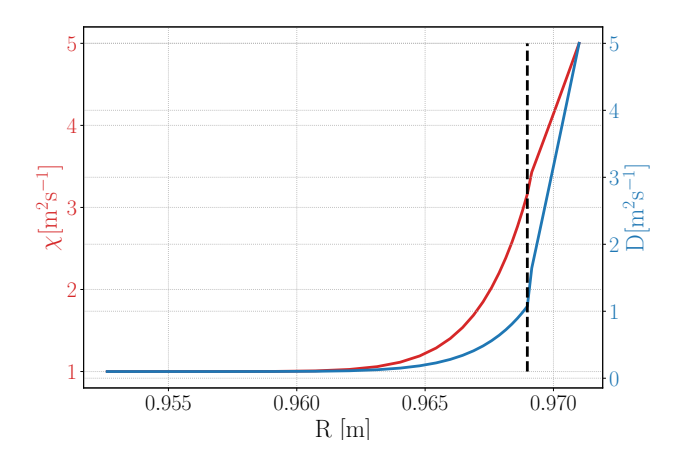


Figure 2: Transport coefficients used in this study, with the separatrix highlighted with a dashed line.

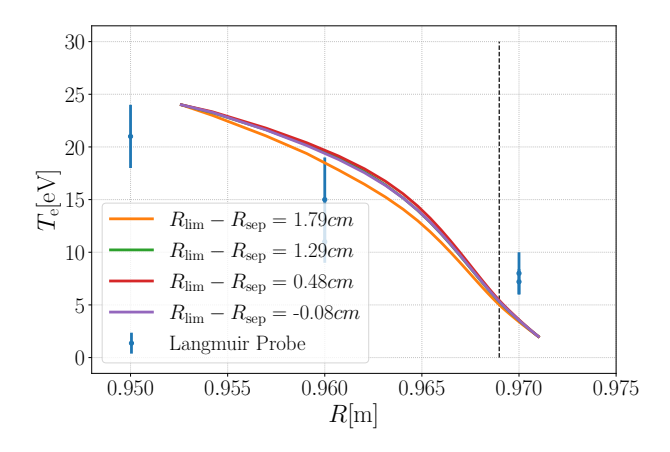
wide wedge limiter and poloidally dependent boundary conditions which are not used in this work. In this work, sputtering results in neutral lithium and sputtering is only due to deuterium flux.

UEDGE is used to find a steady state solution for PI3 shot #18447 at t=5ms. This specific time is typically the most quiescent period for plasmas in PI3, after which an approximation of steady state would fail. We set up our field-aligned mesh based on PI3 #18447 (Fig. 1) with the mesh extending in $\psi/\psi_{\rm sep}$ from 0.925 to 1.011 utilising a Grad–Shafranov (GS) equilibrium generated with CORSICA [25] based on experimental data. We utilize 45 and 30 cells poloidally (inboard and outboard respectively) as well as 30 cells radially. For limited configurations, we refine the mesh around the limiter to reach a resolution of $\Delta x_{\rm guard} < 5 \,\mu{\rm m}$.

A density of $n_{\rm core} = 1.84 \times 10^{19} \, {\rm m}^{-3}$, which is inferred from interferometers, is imposed at the core boundary. We used fixed temperature boundary conditions of $T_e^{\rm inner} = 24 \, {\rm eV}$ and $T_e^{\rm outer} = 4 \, {\rm eV}$ informed by Langmuir probe measurements and from these set the T_i boundary values by an assumption of $T_i \sim 1.3 T_e$ inspired by ion Doppler spectroscopy measurements.

A modest recycling coefficient R=0.75 is used for deuterium, which is higher than the expected recycling coefficient of $R\sim0.5$ reported in LTX- β [26]. However, PI3 discharge 18447 was performed with worn lithium (30 shots after evaporative coating) and thus, we expect the lithium to be significantly passivated and lithium coating variability to be significant. Therefore, we take a conservative estimate of the recycling coefficients in these simulations. We utilise a recycling coefficient of $R=10^{-10}$ for lithium i.e. any ionised lithium that strikes any material surface is effectively absorbed. Evaporation off all surfaces is included. The surface temperature of the walls is set to 293 K and the limiter to 310 K. This is expected to produce little evaporation in practice, but is included for completeness.

We specify spatially dependent particle diffusivity D and electron thermal diffusivity χ_e . The ion thermal diffusivity is



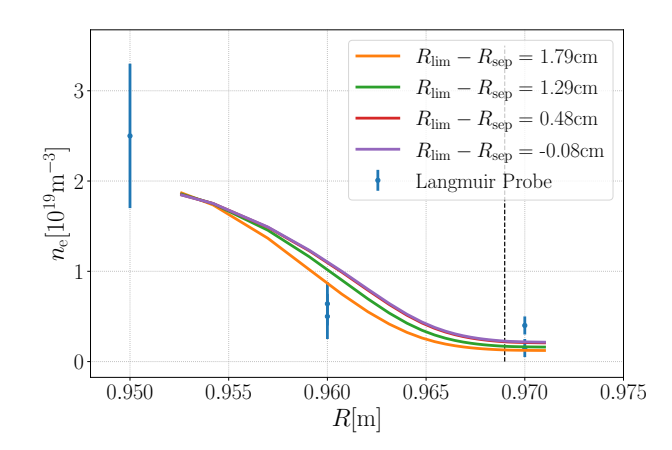
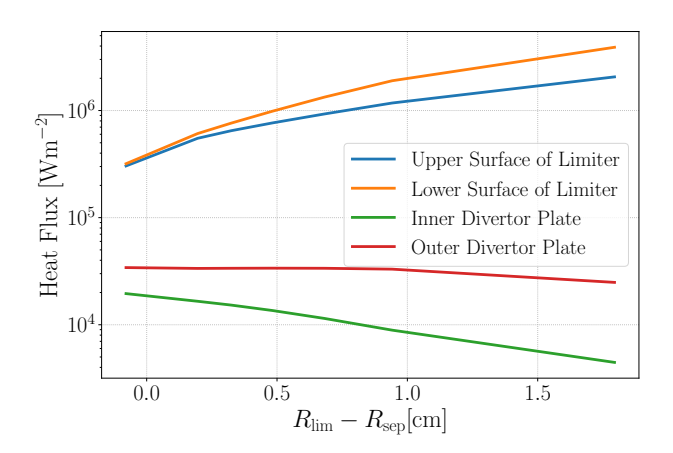


Figure 3: Comparison of three limiter insertion depths compared to measured Langmuir probes data. The separatrix is highlighted with a dashed line, with the edge region left of the separatrix and the SOL to the right, *left*: Electron temperature and *right*: Density.



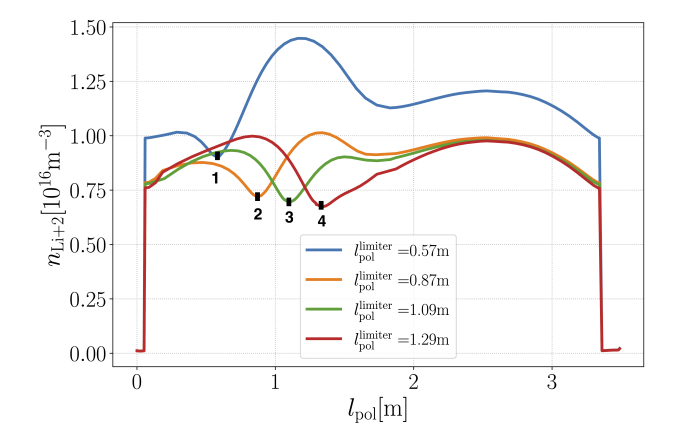


Figure 4: Heat fluxes to the limiter and divertor plates compared with limiter insertion depth.

Figure 5: Li + 2 density along the magnetic surface 4 cells from the core. The black squares indicate the location of the limiter and the numbers correspond to limiter positions in Fig. 1. l_{pol} is the length from the inner divertor plate to the outer.

set to the electron value ($\chi_i = \chi_e$). In this study, we utilise the profile shown in Fig. 2 in an attempt to match the Langmuir probe data at the outer mid-plane. As seen in Fig. 3, we find a good matching of the temperature and density profiles from the Langmuir probe, where Langmuir probe data is collected over multiple shots at similar settings (#18660 - #18669). Shot-to-shot variation is expected, and thus, the discrepancy observed between UEDGE and the Langmuir probe data is within the uncertainty of the experimental data. It is noted that the SOL transport coefficients in this model are the same order as Bohm diffusion ($\sim 3 \text{ m}^2\text{s}^{-1}$).

3. Results and Discussion

The first study compares insertion depth and its effects on the heat fluxes on the limiter and divertor surfaces. Previous work by Rensink and Rognlien [27] showed a clear inverse trend with respect to the insertion depth and heat flux to the divertor plates with an outboard limiter inserted. In this work, we insert the limiter on the inboard side with insertion depth varying from $R_{\rm lim} - R_{\rm sep} = -0.08$ to 1.79 cm, where $R_{\rm lim} - R_{\rm sep}$ is the insertion depth relative to the seperatrix. In this case $R_{\rm lim} - R_{\rm sep} < 0$ cm indicates that the limiter is inserted into the SOL and $R_{\rm lim} - R_{\rm sep} > 0$ cm within the seperatrix. We find a similar trend to Rensink and Rognlien [27] as shown in Fig. 4. Sufficient retraction of the limiter was not performed, and thus the crossing point discussed in [27] is not seen.

However, a notable difference between this study and the work of Rensink [27] is the occurrence of reduced limiter pumping. It is easily seen in Fig. 3 that at the furthest insertion at $R_{\text{lim}} - R_{\text{sep}} = 1.79 \, \text{cm}$ there is a small difference in the density profile. However, it is not as dominant an effect as previously reported. In these simulations, the wall acts as the largest recycling surface, until the limiter dominates at an insertion depth of $R_{\text{lim}} - R_{\text{sep}} > 1.64 \, \text{cm}$, where the limiter determines the density profile. Some effects are observed as early as

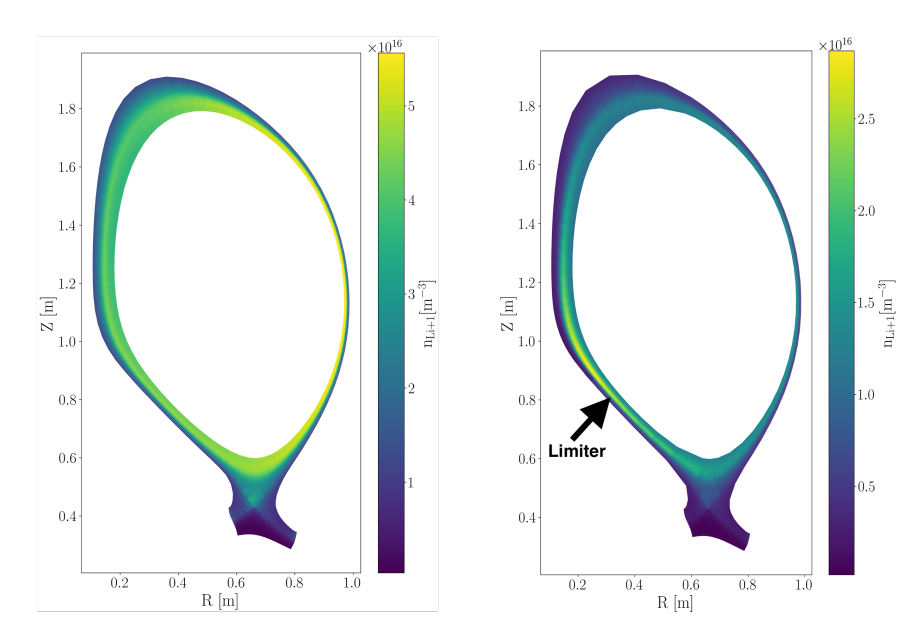


Figure 6: Li + 1 density with left: Diverted and right: Limited plasmas.

 $R_{\rm lim} - R_{\rm sep} = 1.29$ cm but the wall remains the pumping surface from which deuterium ions interact and recycle. This can also be seen comparing the deuterium ion fluxes interacting with the limiter at $R_{\rm lim} - R_{\rm sep} = 0.2$ cm, where the limiter current is 19 A and the wall current is 196 A. As both surfaces have the same recycling coefficient, the density profile is dominated by wall dynamics and not limiter pumping in these instances.

Furthermore, the sputtered lithium transitions from being predominantly sourced from the wall to the limiter as the limiter is inserted further towards the core region. The limiter pumps lithium in the instances of the wall being the source of lithium, and as the limiter is more deeply inserted all material surfaces become important sources of lithium. This can be understood via comparison of neutral lithium current from the wall/limiter for two separate limiter insertions. At $R_{\rm lim}-R_{\rm sep}=0.1$ cm the neutral currents are -0.21 A / -0.1 A, where almost double the lithium is coming from the walls. However, at $R_{\rm lim}-R_{\rm sep}=1.5$ cm the currents are -0.1 A / -3.2 A — a 32 times difference. This is a result from the leading edge being immersed in high energy particles resulting in higher sputtering yield and a larger wetted area.

The second study compares the location of the limiter as varying from position 1 to 4 in Fig. 1 with the limiter inserted into the same flux surfaces. We find that there is poloidal variation in impurity species density as would be expected. We see in Fig. 5 that Li + 2 has a strong dependence on the limiter location in the plasma. This is the case for all species of lithium. The poloidal position (l_{pol}) of the limiter is indicated in these plots by the drop in density as sputtered lithium is primarily neutral or singly ionised near the limiter.

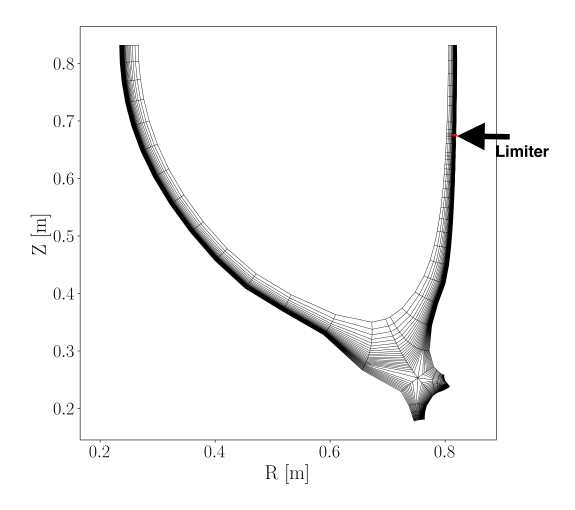
Due to the limiter being on the same flux surface as its position is moved poloidally in the UEDGE mesh, the physical area of the limiter increases as it moves from position 1 to 4 shown in Fig. 1. Further away from the private flux region (position 4) the limiter has the largest wetted area, decreasing as it moves

towards the divertor. This results in the limiter locations having a significant impact on the magnitude of the ionised lithium density. Partly due to parts of the limiter acting to absorb the ionised lithium in the simulation as the recycling coefficient is effectively zero on all surfaces for lithium. Effects resulting from changes in the deuterium density due to limiter pumping will also affect lithium concentration owing to changes in sputtering yield. Thus, a limiter closer to the private flux region results in larger concentration of lithium in the plasma as opposed to a limiter beyond the inner mid-plane.

The final study carried out compares a diverted plasma with no limiter to one with a limiter inserted at position 1 in Fig. 1 and insertion depth of $R_{\rm lim}-R_{\rm sep}=0.45$ cm. Of primary interest is how the heat-fluxes to the various surfaces differ, as well as the behaviour of the impurities and neutrals. It is expected that the heat-flux on the divertor plate closest to the limiter will be significantly lower as seen in the previous study. Indeed, the limiter reduces the heat-flux to the left divertor plate by 62% and the right divertor plate by 40%.

The spatial distribution of lithium is shown in Fig. 6. The diverted configuration has more impurities in the plasma. This is because the wall being a large source of impurities in both cases, but in the limiter case the limiter surface in the SOL acts to reduce the deuterium density and lowers the temperature. As a result, the overall sputtered yield from the walls decrease, reducing the total lithium in the SOL region. In addition, part of the limiter acts as a net sink for the lithium which further decreases the overall lithium in the SOL. This is evident from the low singly ionised lithium density region in Fig. 6, where the entire low-density region is the extent of the limiter. At the leading edge of the limiter, there is a net source of lithium. This is indicated by the localised increase in ionised lithium at the location of the limiter.

Finally, we highlight ongoing work utilising an outboard thin limiter in early design work on a future device for com-



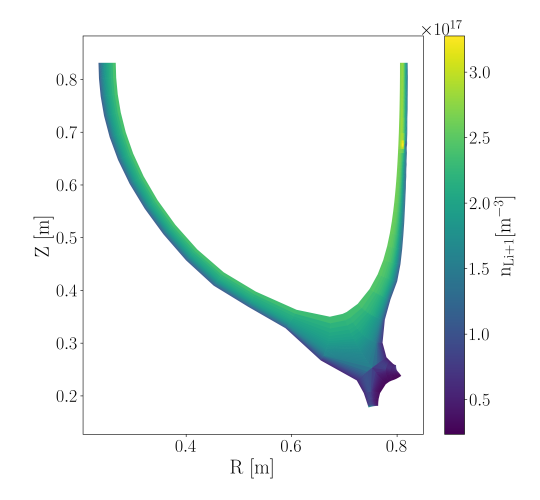


Figure 7: *left*: Mesh for a design stufy of a next-generation plasma compression device in the pre-compressed state mesh with limiter highlighted in red and *right*: Li + 1 density.

pressing spherical tokamak plasmas shown in Fig. 7. In this study, we used an outboard limiter under the assumption that the compressing wall limits the plasma. These models exploit the ability of UEDGE to model an up-down symmetric double-null configuration as a half-domain using a symmetric boundary condition at the equator. The limiter is located at $Z \sim 0.65\,\mathrm{m}$ near the symmetry plane with an insertion depth of $R_{\mathrm{lim}}-R_{\mathrm{sep}}=-0.25\,\mathrm{cm}$, which in this case is 0.25 cm into the core region. Expected lithium behaviour is observed in Fig. 7, with a maxima local to the limiter tip. This suggests that the limiter application is physically reasonable in this novel geometry as well, and future design studies can be carried out to minimise lithium ingress using a limiter.

4. Summary and conclusions

The first edge plasma calculations of PI3 have been conducted in the regime of a diverted plasma and with a limiter inserted, in the presence of solid lithium surfaces. We found that limiter insertion depth was a key parameter in determining heat fluxes to the divertor plates. As the limiter was inserted past the separatrix, the heat fluxes to the limiter increased and the divertor heat fluxes decreased in agreement with previous work [27]. The primary particle fluxes were to the walls and the wall was the primary pumping surface. This was unlike what was reported in [27] where the limiter had a large impact on the density profile, a behaviour that was found in this work only after deep insertion of the limiter.

In addition, we found that the location of the limiter determined the impurity distribution. As the limiter was moved away from the private flux region the impurity densities reduced due to changes in the plasma wetted area seen by the plasma. At position 4, the wetted area was the largest and therefore resulted in a reduction in lithium as the limiter due to a reduction a reduction in sputtering yield as well as parts of the limiter acting as

sink. This trend continued in an anti-clockwise direction with increasing lithium concentration.

Furthermore, it was found that the insertion of the limiter compared to a fully diverted plasma caused a reduction of heat fluxes by 62% and 40% to the left and right divertor plates. However, the diverted plasmas had significantly more impurities present due to the wall being a large source of impurities with no sinks near the core plasma. Whereas, the limiter acted to decrease lithium density via reducing the deuterium density in the SOL resulting in a decreased sputtering yield. In addition, the limiter acted as a sink on parts of it surfaces to lithium reducing the overall lithium in the plasma further.

Finally, we highlighted the use of a thin limiter on the outboard side for a novel device currently being designed. The outboard limiter resulted in physically reasonable behaviour suggesting that UEDGE is capable and applicable for future design studies of the plasma compression device.

Future work involves utilising more accurate boundary conditions representing the power entering the plasma. In addition, exploring the effects of the recycling coefficient is of key interest at General Fusion and how that affects the edge region. The final aim is to extend all this to a compressing spherical tokamak design study.

Acknowledgements

We thank the experimental group at General Fusion for the experimental results. Performed in part by LLNL under Contract DE-AC52-07NA27344 in support of General Fusion under SPP-L23083. This work was supported by funding from the Government of Canada through its Strategic Innovation Fund (Agreement No. 811-811346). The funding source had no involvement in: the study design; the collection, analysis and interpretation of data; the writing of the report; the decision to submit the article for publication.

Author Contributions

Abetharan Antony: Conceptualization, Investigation, Visualization, Methodology, Formal Analysis, Writing - Original Draft. Leopoldo Carbajal: Software, Methodology, Writing - Review & Editing. Tom Rognlien: Conceptualization, Software, Methodology, Supervision, Writing - Review & Editing. Maxim Umansky: Conceptualization, Software, Supervision, Writing - Review & Editing. Aaron Froese: Resources, Writing - Review & Editing. Colin McNally: Supervision, Writing - Review & Editing. Stephen Howard: Resources, Writing - Review & Editing. Celso Ribeiro: Resources. Russ Ivanov: Resources. Carl Dunlea: Resources.

References

- M. Laberge, Magnetized Target Fusion with a Spherical Tokamak, Journal of Fusion Energy 38 (1) (2019) 199–203. doi:10.1007/s10894-018-0180-3.
- [2] L. Carbajal, S. Jones, M. Reynolds, Z. Seifollahi Moghadam, A. Mossman, Modeling and simulation of lithium transport and radiation in diverted Pi3 plasmas, Physics of Plasmas 30 (7) (2023) 072503. arXiv:https://pubs.aip.org/aip/pop/articlepdf/doi/10.1063/5.0153107/18029932/072503_1_5.0153107.pdf, doi:10.1063/5.0153107.
 - URL https://doi.org/10.1063/5.0153107
- [3] S. I. Krasheninnikov, L. E. Zakharov, G. V. Pereverzev, On lithium walls and the performance of magnetic fusion devices, Physics of Plasmas 10 (2003) 1678–1682. doi:10.1063/1.1558293.
- [4] T. D. Rognlien, M. E. Rensink, Impurity transport in edge plasmas with application to liquid walls, Physics of Plasmas 9 (5) (2002) 2120–2126. doi:10.1063/1.1461384.
- [5] M. G. Bell, H. W. Kugel, R. Kaita, L. E. Zakharov, H. Schneider, B. P. Leblanc, D. Mansfield, R. E. Bell, R. Maingi, S. Ding, S. M. Kaye, S. F. Paul, S. P. Gerhardt, J. M. Canik, J. C. Hosea, G. Taylor, Plasma response to lithium-coated plasma-facing components in the National Spherical Torus Experiment, Plasma Physics and Controlled Fusion 51 (12) (2009). doi:10.1088/0741-3335/51/12/124054.
- [6] J. M. Canik, R. Maingi, S. Kubota, Y. Ren, R. E. Bell, J. D. Callen, W. Guttenfelder, H. W. Kugel, B. P. Leblanc, T. H. Osborne, V. A. Soukhanovskii, Edge transport and turbulence reduction with lithium coated plasma facing components in the National Spherical Torus Experiment, Physics of Plasmas 18 (5) (2011). doi:10.1063/1.3592519.
- [7] R. Maingi, J. M. Canik, R. E. Bell, D. P. Boyle, A. Diallo, R. Kaita, S. M. Kaye, B. P. LeBlanc, S. A. Sabbagh, F. Scotti, V. A. Soukhanovskii, Effect of progressively increasing lithium conditioning on edge transport and stability in high triangularity NSTX H-modes, Fusion Engineering and Design 117 (2017) 150–156. doi:10.1016/j.fusengdes.2016.06.058. URL http://dx.doi.org/10.1016/j.fusengdes.2016.06.058
- [8] R. Majeski, R. E. Bell, D. P. Boyle, R. Kaita, T. Kozub, B. P. LeBlanc, M. Lucia, R. Maingi, E. Merino, Y. Raitses, J. C. Schmitt, J. P. Allain, F. Bedoya, J. Bialek, T. M. Biewer, J. M. Canik, L. Buzi, B. E. Koel, M. I. Patino, A. M. Capece, C. Hansen, T. Jarboe, S. Kubota, W. A. Peebles, K. Tritz, Compatibility of lithium plasma-facing surfaces with high edge temperatures in the lithium tokamak experiment, Physics of Plasmas 24 (2017) 056110. doi:10.1063/1.4977916.
- [9] D. P. Boyle, R. Majeski, J. C. Schmitt, C. Hansen, R. Kaita, S. Kubota, M. Lucia, T. D. Rognlien, Observation of flat electron temperature profiles in the lithium tokamak experiment, Physical Review Letters 119 (7 2017). doi:10.1103/PhysRevLett.119.015001.
- [10] G. Z. Zuo, J. S. Hu, J. G. Li, Z. Sun, D. K. Mansfield, L. E. Zakharov, Lithium coating for H-mode and high performance plasmas on EAST in ASIPP, Journal of Nuclear Materials 438 (SUPPL) (2013) 90–95. doi:10.1016/j.jnucmat.2013.01.014.
- [11] T. Xie, S. Y. Dai, G. Z. Zuo, L. Wang, H. M. Zhang, B. Lyu, L. Zhang, J. Huang, J. S. Hu, Y. Feng, D. Z. Wang, EMC3-EIRENE modelling of edge plasma and impurity emissions compared with the liquid lithium

- limiter experiment on EAST, Nuclear Fusion 58 (10) (2018) 106017. doi:10.1088/1741-4326/aad42f.
- [12] T. Xie, S. Y. Dai, Z. Sun, G. Z. Zuo, J. S. Hu, Y. Feng, D. Z. Wang, Investigation of edge impurity transport and divertor fluxes by toroidally localized lithium injection on EAST with EMC3-EIRENE, Plasma Physics and Controlled Fusion 61 (11) (2019). doi:10.1088/1361-6587/ab434a.
- [13] F. Scotti, V. A. Soukhanovskii, R. E. Bell, S. Gerhardt, W. Guttenfelder, S. Kaye, R. Andre, A. Diallo, R. Kaita, B. P. Leblanc, M. Podestá, Core transport of lithium and carbon in elm-free discharges with lithium wall conditioning in NSTX, Nuclear Fusion 53 (2013). doi:10.1088/0029-5515/53/8/083001.
- [14] D. P. Boyle, Measurements of impurity concentrations and transport in the lithium tokamak experiment, Ph.D. thesis, Princeton University: Plasma Physics Department (2016).
- [15] W. A. Houlberg, K. C. Shaing, S. P. Hirshman, M. C. Zarnstorff, Boot-strap current and neoclassical transport in tokamaks of arbitrary collisionality and aspect ratio, Physics of Plasmas 4 (9) (1997) 3230–3242. arXiv:https://doi.org/10.1063/1.87246, doi:10.1063/1.872465.
- [16] E. A. Belli, J. Candy, Kinetic calculation of neoclassical transport including self-consistent electron and impurity dynamics, Plasma Physics and Controlled Fusion 50 (9) (2008) 095010. doi:10.1088/0741-3335/50/9/095010.
- [17] R. A. Hulse, Numerical studies of impurities in fusion plasmas, Nuclear Technology Fusion 3 (2) (1983) 259–272. arXiv:https://doi.org/10.13182/FST83-A20849, doi:10.13182/FST83-A20849.
- [18] J. Lore, J. Canik, Y. Feng, J.-W. Ahn, R. Maingi, V. Soukhanovskii, Implementation of the 3d edge plasma code emc3-eirene on nstx, Nuclear Fusion 52 (5) (2012) 054012. doi:10.1088/0029-5515/52/5/054012.
- [19] T. Rognlien, J. Milovich, M. Rensink, G. Porter, A fully implicit, time dependent 2-d fluid code for modeling tokamak edge plasmas, Journal of Nuclear Materials 196-198 (1992) 347–351, plasma-Surface Interactions in Controlled Fusion Devices. doi:https://doi.org/10.1016/S0022-3115(06)80058-9.
 - URL https://www.sciencedirect.com/science/article/pii/S002231150
- [20] R. Schneider, X. Bonnin, K. Borrass, D. P. Coster, H. Kastelewicz, D. Reiter, V. A. Rozhansky, B. J. Braams, Plasma edge physics with B2-Eirene, Contributions to Plasma Physics 46 (2006) 3–191. doi:10.1002/ctpp.200610001.
- [21] D. Reiter, M. Baelmans, P. Börner, The EIRENE and B2-EIRENE codes, Fusion Science and Technology 47 (2) (2005) 172–186. doi:10.13182/FST47-172.
- [22] D. Stotler, C. Karney, Neutral gas transport modeling with degas 2, Contributions to Plasma Physics 34 (2-3) (1994) 392–397. arXiv:https://onlinelibrary.wiley.com/doi/pdf/10.1002/ctpp.2150340246, doi:https://doi.org/10.1002/ctpp.2150340246.
- [23] D. J. Battaglia, K. H. Burrell, C. S. Chang, S. Ku, J. S. Degrassie, B. A. Grierson, Kinetic neoclassical transport in the H-mode pedestal, Physics of Plasmas 21 (7) (2014). doi:10.1063/1.4886803.
- [24] T. D. Rognlien, D. D. Ryutov, N. Mattor, G. D. Porter, Two-dimensional electric fields and drifts near the magnetic separatrix in divertor tokamaks, Physics of Plasmas 6 (5 I) (1999) 1851–1857. doi:10.1063/1.873488.
- [25] J. Crotinger, L. LoDestro, L. Pearlstein, A. Tarditi, T. Casper, E. Hooper, Llnl report ucrl-id-126284, NTIS# PB2005-102154 (1997).
- [26] A. Maan, D. P. Boyle, R. Majeski, G. J. Wilkie, M. Francisquez, S. Banerjee, R. Kaita, R. Maingi, B. P. LeBlanc, S. Abe, E. Jung, E. Perez, W. Capecchi, E. T. Ostrowski, D. B. Elliott, C. Hansen, S. Kubota, V. Soukhanovskii, L. Zakharov, Estimates of global recycling coefficients for LTX-β discharges, Physics of Plasmas 31 (2) (2024) 022505. arXiv:https://pubs.aip.org/aip/pop/article-pdf/doi/10.1063/5.0177604/19676596/022505_1_5.0177604.pdf, doi:10.1063/5.0177604.
 - URL https://doi.org/10.1063/5.0177604
- 27] M. Rensink, T. Rognlien, Edge plasma modeling of limiter surfaces in a tokamak divertor configuration, Journal of Nuclear Materials 266-269 (1999) 1180-1184. doi:https://doi.org/10.1016/S0022-3115(98)00859-9. URL https://www.sciencedirect.com/science/article/pii/S002231158